[Frontiers in Bioscience E2, 231-240, January 1, 2010]

PE-CMOS based C-scan ultrasound for foreign object detection in soft tissue

Chu-Chuan Liu[1, 2], Shih-Chung Ben Lo[1], Matthew T Freedman[1], Marvin E Lasser[3], John Kula[3], Anita Sarcone[1], Yue Wang[2]

[1]Imaging Science and Information Systems Center, Georgetown University Medical Center, Washington, DC 20057, USA, [2] Bradley Department of Electrical and Computer Engineering, Virginia Polytechnic Institute and State University, Arlington, VA 22203, USA, [3] Imperium Inc., Silver Spring, MD 20903, USA

TABLE OF CONTENTS

1. ABSTRACT

In this paper, we introduce a C-scan ultrasound prototype and three imaging modalities for the detection of foreign objects inserted in porcine soft tissue. The object materials include bamboo, plastics, glass and aluminum alloys. The images of foreign objects were acquired using the C-scan ultrasound, a portable B-scan ultrasound, film-based radiography, and computerized radiography. The C-scan ultrasound consists of a plane wave transducer, a compound acoustic lens system, and a newly developed ultrasound sensor array based on the complementary metal-oxide semiconductor coated with piezoelectric material (PE-CMOS). The contrast-to-noise ratio (CNR) of the images were analyzed to quantitatively evaluate the detectability using different imaging modalities. The experimental results indicate that the C-scan prototype has better CNR values in 4 out of 7 objects than other modalities. Specifically, the C-scan prototype provides more detail information of the soft tissues without the speckle artifacts that are commonly seen with conventional B-scan ultrasound, and has the same orientation as the standard radiographs but without ionizing radiation.

2. INTRODUCTION

Penetrating trauma with retained foreign matter is commonly seen in emergency medical departments and in battlefield casualties. The inability to detect and remove foreign objects may lead to serious infection, inflammation or other possible complications. For injured patients, identification and localization of foreign objects are essential to facilitate the removal and treatment. Imaging modalities such as conventional radiography (1) and B-scan ultrasound (2-4) are commonly used for detecting the location, size and shape of the foreign object. Radiologist then identifies a foreign object by distinguishing its different radiodensity (or echo pattern in B-scan ultrasound) from that of the surrounding normal tissue. Once identified, localization for removal remains challenging; radiographs are usually done in a separate facility, limiting interactive wound cleaning and imaging; conventional ultrasound images require that the foreign matter presents a surface perpendicular to the ultrasonic beam.

We have previously reported that C-scan ultrasound can assist in guiding core biopsy, cyst drainage

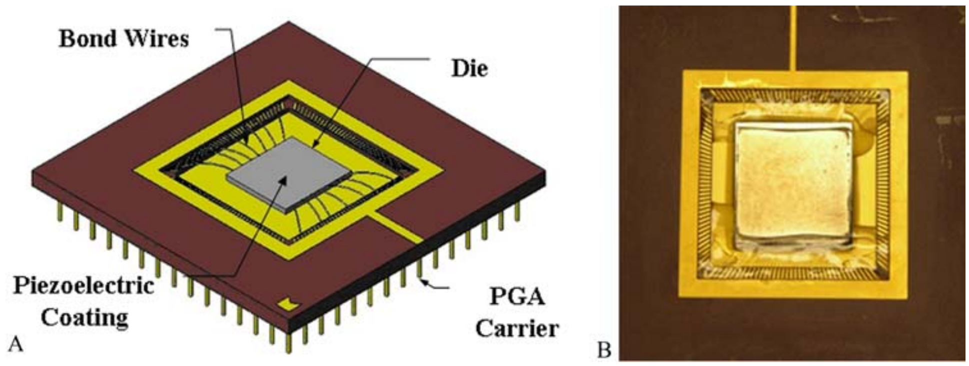

Figure 1. (a) Diagram of the PE-CMOS sensor array. (b) A photograph of the chip.

and the visualizing bone fractures (5-7). Unlike conventional B-scan ultrasound which provides a cross-sectional image in the x and z (depth) directions, the C-scan imaging system produces images in the x-y plane, and does not require restricted pulse-echo orientations (when operating a B-scan probe, the pulse-echo orientation must remain perpendicular to the imaging target, otherwise the echo of the object will "disappear" from the display image due to misalignment of the scanning signal angle and the angle for detecting the echo). In addition, instead of repeated angular shift of the transducer as is done with B-mode ultrasound to find the reflection signal, C-scan ultrasound provides the scanning capability without moving the transducer. Lastly, the varying pressure applied with B-mode transducer may cause foreign object to shift location; while with C-scan the chance of lesion shift from the field of view is less.

In this study, we compared a novel C-scan ultrasound imaging prototype (Imperium Inc., Silver Spring, MD) with three conventional imaging modalities in their capability of detecting foreign objects contained in soft tissue. Foreign objects, made of varying materials including bamboo, plastics, glass, and aluminum alloys, were inserted into a slab of pork with skin, fat, and muscle tissues. Each object was individually inserted into the skin, passed through the fat layer, and penetrated into the muscle layer of the porcine tissue sample. Images of the porcine tissue sample were taken using the C-scan prototype, a portable B-scan ultrasound, a film-based radiography, and a computerized radiography (CR). We then computed the contrast-to-noise ratio (CNR) for each object in the soft tissue to evaluate the performance of the C-scan prototype against other imaging modalities.

3. MATERIAL AND METHODS

3.1. PE-CMOS sensor array

The C-scan ultrasound imaging prototype used in this study consists of three major components: a plane wave ultrasound transducer operating at 5MHz, a compound acoustic lens system, and an ultrasound sensor array using piezoelectric sensing complementary metal-oxide semiconductor (PE-CMOS) technology. The two-dimensional sensor has 128 × 128 pixel elements on a 1cm × 1cm area with 85 microns center-to-center spacing. A schematic diagram and a photograph of this PE-CMOS array sensor are shown in Figure 1A and Figure 1B, respectively. The detailed structures of this array consist of piezoelectric material which is deposited onto a silicon readout multiplexer through semiconductor processing, and a transducer array that is made by spin-coating a pre-selected read-out integrated circuit (ROIC) array with approximately 10 microns thick polyvinylidene difluoride (PVDF) copolymer. This PE-CMOS sensor array is responsive to a wide range of ultrasound frequencies from ~3KHz to ~25MHz (Figure 2). Developments in the advanced acoustic science and sensor technology make this state-of-the-art sensor array applicable to the ultrasound imaging in the projection geometry.

3.2. Compound acoustic lens system

In order to focus the incident ultrasound energy and project the entire field of view over the surface of the PE-CMOS sensor array, a compound acoustic lens system is employed. The two pieces of lenses are specially designed for this PE-CMOS sensor array by Ultra-Acoustics, Inc. (Woodstock, GA) when the ultrasound transducer is operated at 1MHz~10MHz. Figure 3 illustrates a ray tracing diagram of the compound lens system while a parallel ultrasound beam is used. Both lenses are made of Styraclear with refractive index of 0.63 and have the identical size of 7.0cm in diameter. The fixed distance between the front flat lens surface and the sensor array is 8.6cm. To change the focus, the rear lens can be moved forward/ backward with the sensor array fixed at the same place.

3.3. Concept of the ultrasound C-scan Imaging

Based on the physical characteristics of ultrasound, the projection imaging system has been developed as illustrated in Figure 4. In the projection geometry, the imaging object is placed between the transducer and receiver. The emitted ultrasound energy generated from the unfocused transducer is attenuated inside the object; then, the acoustic lens system collects the transmitted-scattered energy and focuses it onto the 2D sensor. The receiving ultrasound energy is further processed by a standard video device for real-time display. Figure 5 gives a photograph of the laboratory C-scan prototype with arrows indicating the major components. In

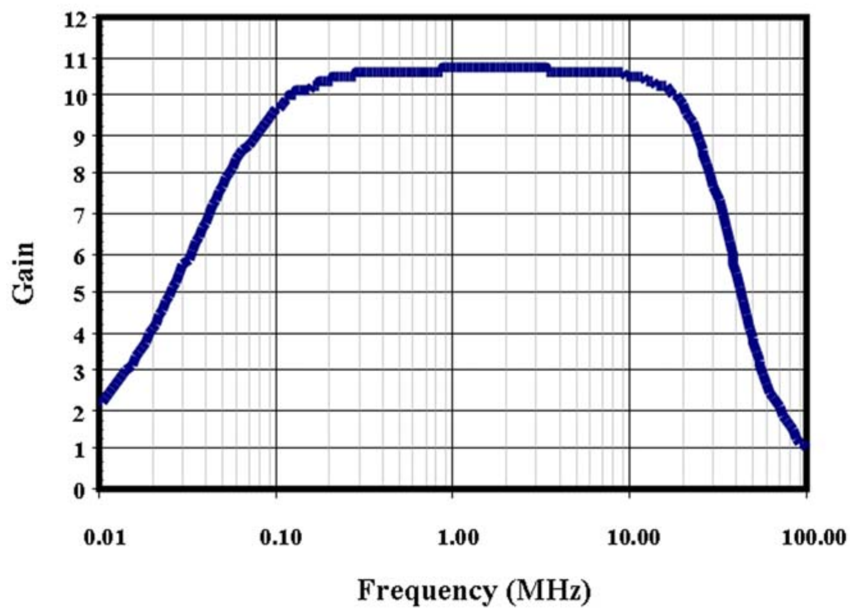

Figure 2. The frequency responsive range of this array.

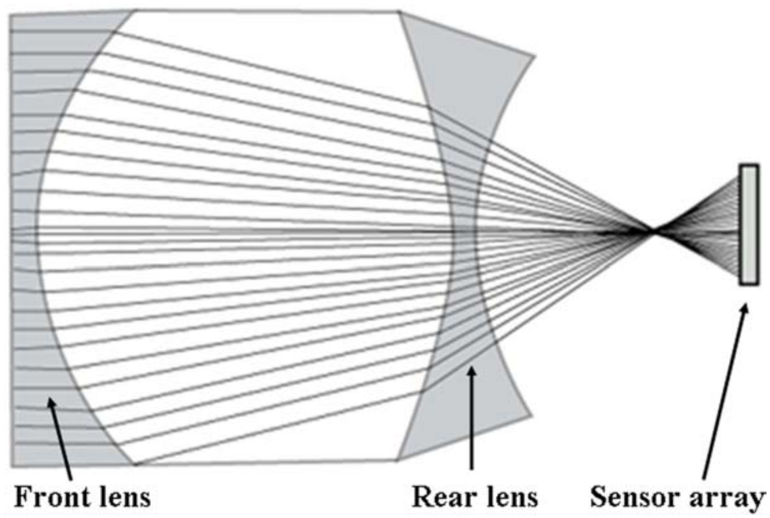

Figure 3. A diagram showing ray tracing of the ultrasound with the compound lens when a parallel beam is used.

preliminary investigations, we found that the C-scan imaging prototype can generate real-time, non-distorted and speckle-free ultrasound images with a spatial resolution of ~350 microns and dynamic range at ~70dB (5,6). This system can also be adapted to perform ultrasound *Computerized Tomography* (US-CT) for imaging small objects when multiple views are acquired (8,9).

3.4. Soft tissue and foreign objects

In this comparative study, four imaging modalities were used to evaluate their ability to detect foreign objects in soft tissue. The selected porcine tissue sample was a slab of pork consisting of skin, fat, and muscle layers (Figure 6). The dimensions of the sample are ~10cm (L) × ~5cm (W) × ~2.5cm (H). The average sound speed for the porcine soft tissue is close to water: skin (~1500m/s), fat (~1430m/s), and muscle (~1580m/s) (10). Their corresponding attenuation coefficients are: skin (2-4dB/cm/MHz), fat (0.8dB/cm/MHz) and muscle (0.5-1.5dB/cm/MHz) (11).

To better simulate injured soft tissue due to forceful penetration, seven foreign objects were inserted into the porcine soft tissue sample from the skin, passed through the fat tissue, and penetrated into the muscle layer. The insertion process was conducted in a container of water to prevent air bubbles. Figure 7 illustrates the seven foreign objects employed in the experiment including one bamboo

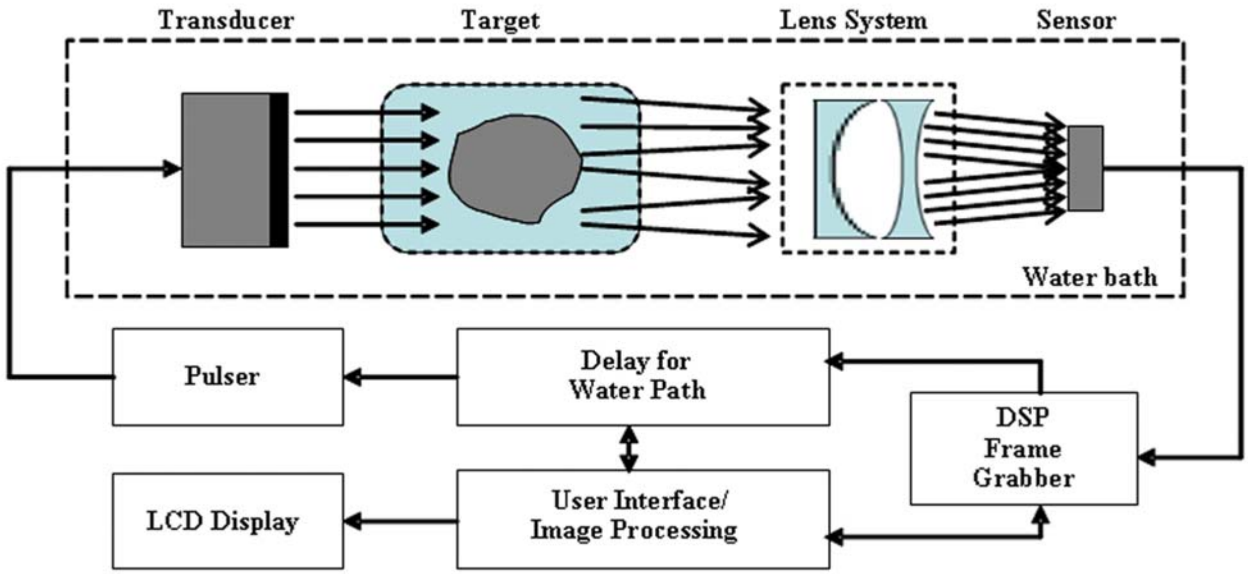

Figure 4. Schematic diagram of the C-scan ultrasound imaging geometry.

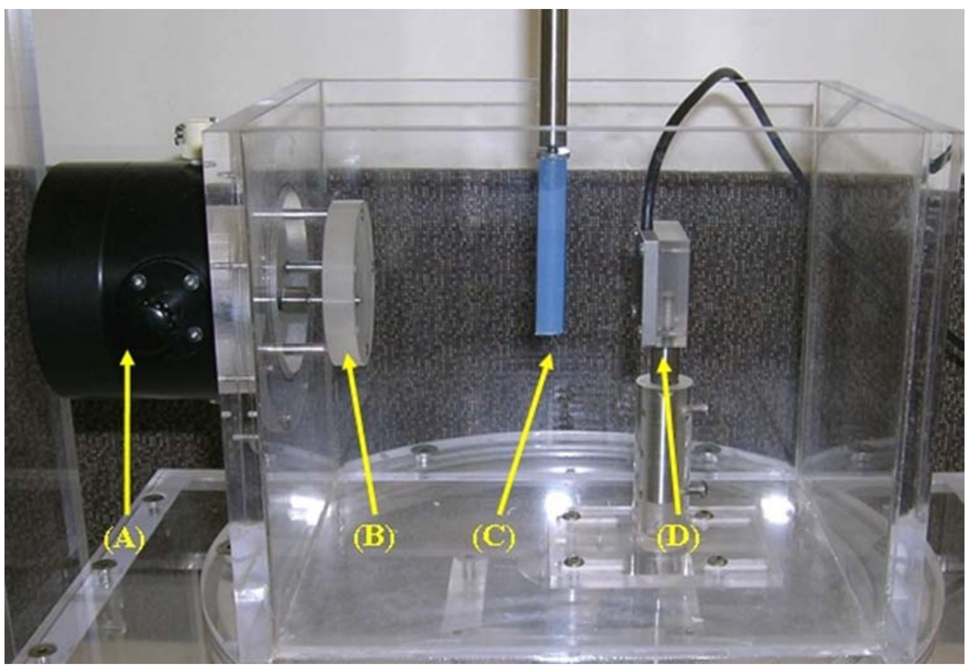

Figure 5. A photograph of the of the C-scan prototype. Arrows represents the locations of major components of the prototype (left to right): (A) the sensor unit is directly mounted on the left side of the water tank, (B) acoustic lens system, (C) the imaging target, and (D) the plane-wave transducer.

object, three kinds of plastic objects, one glass object and two aluminum alloy objects with different shapes and sizes. Object No.1 is a bamboo skewer. Plastic objects No.2, No.3 and No.7 are made of heavy-weight polystyrene, nylon and extra heavy-weight polystyrene, respectively. The glass object (No.6) is obtained from a broken light bulb. Metal objects are made of aluminum alloys of 5182 (No.4) and 3104 (No.5) series. The thicknesses of these objects vary from 0.01 cm to 0.25 cm. Dimensions of these objects and their corresponding acoustic properties are listed in Table 1. Note that objects with unknown attenuation information were computed by the average intensity loss between their individual C-scan image and the initial image acquired

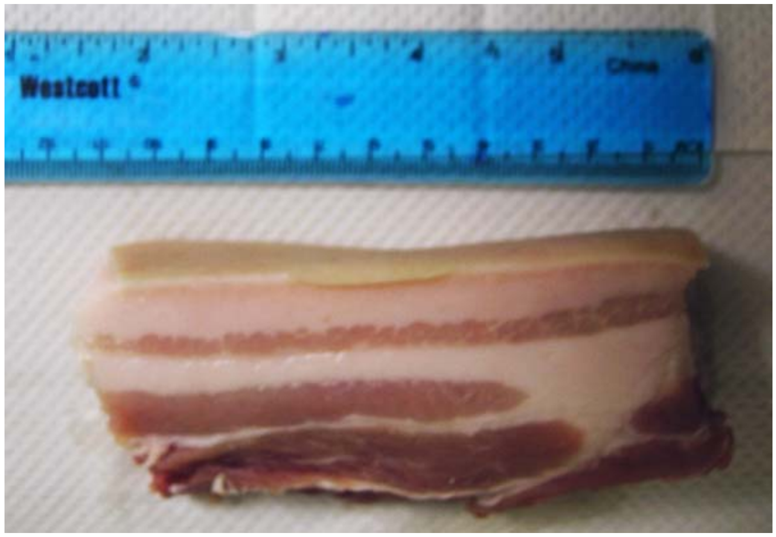

Figure 6. The soft tissue sample is composed of skin, fat, and muscle tissues.

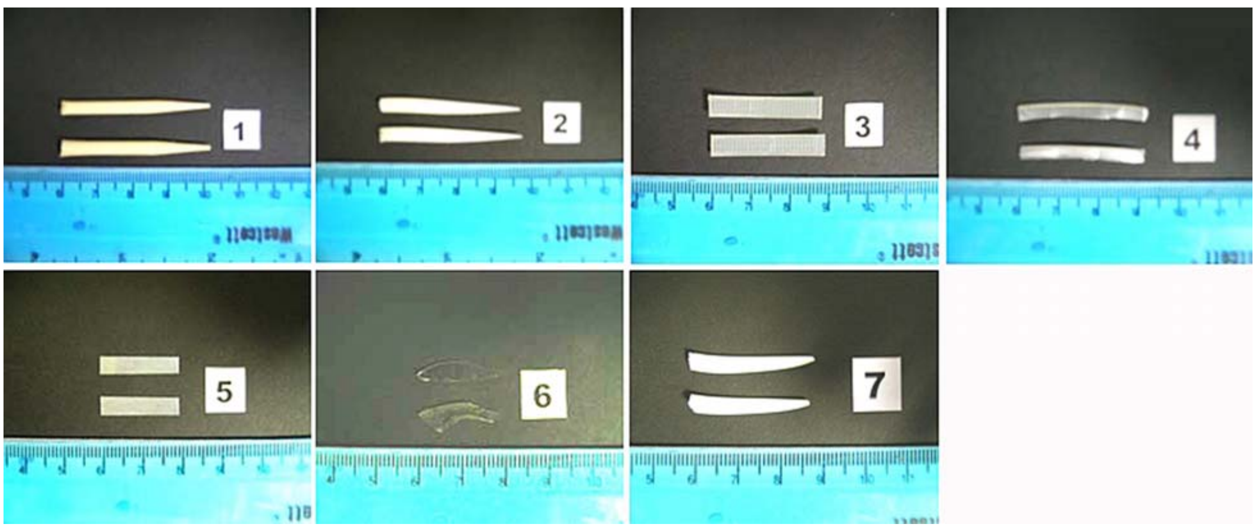

Figure 7. The foreign objects used in the experiment: objects of No.1 are bamboo skewers; Nos. 2, 3, and 7 are plastic sticks; Nos. 4 and 5 are aluminum alloys; No.6 are pieces of glass. Note that only one object in each category was selected.

without target (i.e. water only). The attenuation coefficient was calculated by

$$\alpha = -10 \cdot \log_{10}\left(\frac{I_d}{T_{t,w}^2 \cdot I_0}\right) / x \qquad (1)$$

and

$$T_{t,w} = \frac{4 Z_t Z_w}{(Z_t + Z_w)^2} \qquad (2)$$

where α represents the attenuation coefficient in Decibel (dB), I_d is the target's average intensity in the C-scan image, I_0 is the initial intensity obtained without target, and x is the average thickness of the target. $T_{t,w}$ represents the intensity transmission coefficient which is a function of the acoustic impedances of the target (Z_t) and water (Z_w).

3.5. Imaging orientation

The same porcine soft tissue sample, containing the foreign objects, was imaged by the C-scan ultrasound prototype operated at 5MHz and three other imaging modalities including a portable B-scan ultrasound imaging system (Terason Ultrasound System with curved linear 4C2 wideband 128 elements probe operated at 4MHz), a film-based radiography system operated at 44kVP, and a CR system operated at 40kVP. All images were obtained using a perpendicular viewing orientation in order to cover most of the foreign objects in the same view (Figure 8).

4. RESULTS

4.1. C-scan ultrasound images

The image characteristic of C-scan ultrasound is different from other imaging modalities, e.g. radiography

Table 1. Parameters and acoustic properties of test objects

Object	No.1	No.2	No.3	No.4	No.5	No.6	No.7
Material	bamboo	heavy-weight polystyrene	nylon	aluminum alloy-5182	aluminum alloy-3104	glass	extra heavy-weight polystyrene
Thickness (cm)	0.25	0.15	0.1	0.1	0.01	0.1	0.2
Length (cm)	4	4	3	3	2	2	2.5
Width (cm)	0.2	0.15	0.3	0.2	0.3	0.2	0.25
Density[a] (g/cm^3)	0.9	1.05	1.12	2.65	2.72	2.2	1.04
Average Sound Speed[1] (m/s)	5600	2400	2600	6500	6320	5900	2320
Attenuation[1] (dB/cm @ 5MHz)	19.0[2,3]	1.8	2.9	14.2[2]	14.1[2]	12.5[2]	3.6

[1] From Selfridge (12) and Wegst (13), [2] Experimental data computed by using the C-scan prototype, [3] Approximate value with air contained inside its fibrotic structure

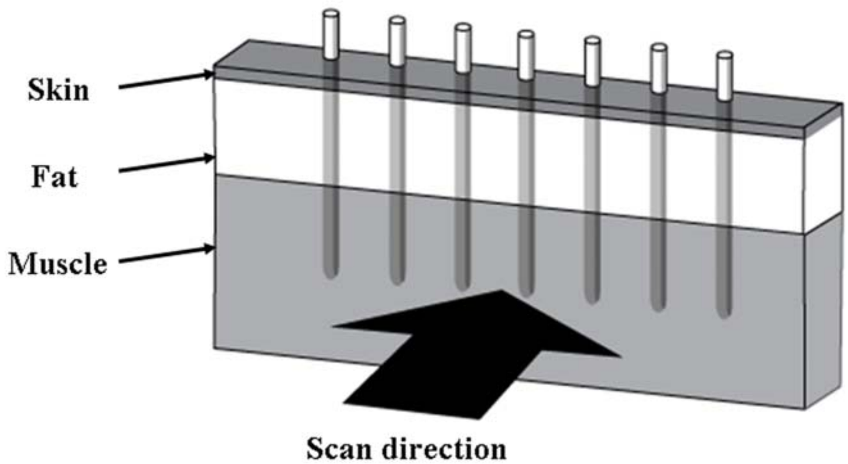

Figure 8. The imaging direction for all image modalities is perpendicular to the inserting direction.

and B-scan ultrasound. When the object has higher attenuation properties, it appears darker in the C-scan image because more ultrasound energy is attenuated within the object; thus, less energy passes through to the receiver.

In this experiment, a 5MHz transducer was employed to acquire ultrasound images of the porcine tissue sample using the C-scan prototype. Figure 9 shows a series of the C-scan images with each centered at a foreign object. The C-scan images revealed that most of foreign objects were observable. In addition, the structural features of fat and muscle tissues were clearly captured in the C-scan images.

In order to view the C-scan image of the whole area containing the foreign objects, standard image stitching processes were performed to combine these C-scan images (Figure 10). The stitched C-scan image facilitates visual comparisons with the images obtained from other modalities.

4.2. B-scan ultrasound images

The B-scan ultrasound images were acquired by placing the probe to the side of the porcine tissue sample using the portable device operating at 4 MHz. Figure 11 shows two image sections of the porcine tissue sample. It can be seen that the bamboo skewer, plastic objects, and the glass piece are observable; however, edges of objects are not due to small cross-sectional size of the object and speckle artifacts. The metal object (No.5) is only apparent in one of the B-scan images due to its tilt orientation.

4.3. Film-based radiograph and computerized radiography (CR) image

The same porcine tissue sample was then imaged by two radiography systems. Figure 12A illustrates the film-based radiograph of the porcine tissue obtained at 44kVP and Figure 12B shows the CR image obtained at 40kVP. The thicker metal piece and the glass piece are the most visible in both the radiographs. For the aluminum alloy pieces (No. 4 and 5), the CR image shows better contour than the film-based radiograph. The bamboo skewer and plastic sticks are barely observable in either the film-based radiographs or CR images except the portions outside of the porcine tissue sample that are surrounded by air.

4.4. Visual comparison of the C-scan images and the radiographs

Although C-scan ultrasound and radiography systems use similar imaging geometries, their intensity representations are different. The foreign objects are represented with higher gray levels (brighter) in the radiographs rather than the lower gray levels (darker) in the C-scan attenuation images. For better visual comparison, we inverted the intensity of the C-scan images and placed them above the radiographs. Figure 13A shows the intensity inverted C-scan image and the film-based radiograph; Figure 13B shows the intensity inverted C-scan image and the CR image. The arrows connected to each number point out the same object in both images. The comparison images illustrate that both the bamboo skewer and plastic objects in the C-scan images are more conspicuous than those in the radiographs.

Table 2. CNR values of each foreign object for all imaging modalities

Object	No.1	No.2	No.3	No.4	No.5	No.6	No.7
Material	bamboo	heavy-weight polystyrene	nylon	aluminum alloy-5182	aluminum alloy-3104	glass	extra heavy-weight polystyrene
C-scan Ultrasound	**3.80**	**2.17**	1.71	**8.62**	1.1	7.51	**1.76**
B-scan Ultrasound	2.08	1.25	**4.09**	3.84	1.79	1.77	0.47
Film-Based Radiography	1.1	0.2	0.57	7.6	1.12	**8.43**	0.42
Computerized Radiography	0.2	0.39	0.45	7.27	**3.46**	8.04	0.62

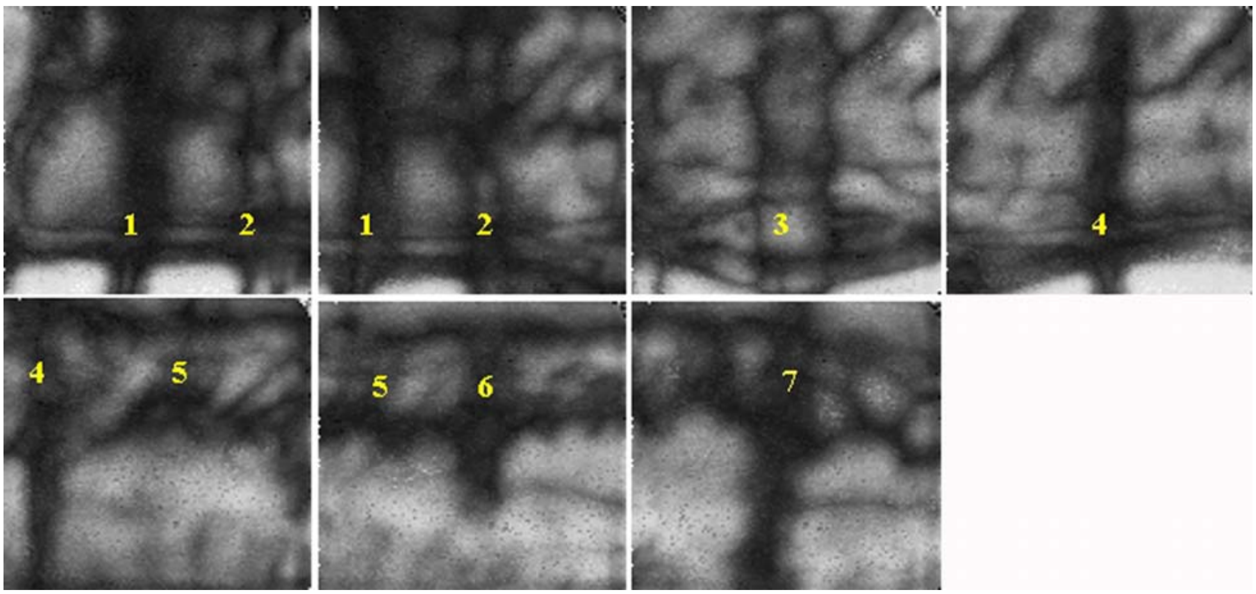

Figure 9. A series of C-scan images for the foreign objects contained in the porcine tissue sample. The bold numbers indicate the specific foreign object according to Table 1.

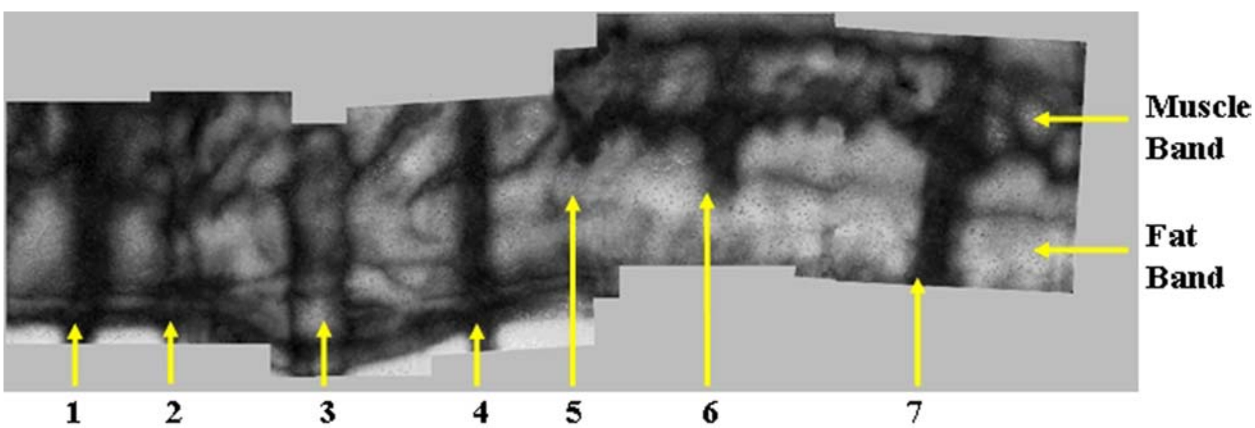

4.5. Contrast-to-noise ratio analyses

We further analyzed the detectability of the object image by computing the contrast-to-noise ratio (CNR) for each foreign object within the porcine tissue sample per modality:

$$CNR = \frac{(f_m - b_m)}{\sqrt{(\sigma_f^2 + \sigma_b^2)/2}} \quad (3)$$

where f_m and b_m are mean intensity values of foreground and background in the image, respectively. The quantities of σ_f and σ_b are the corresponding standard deviations. The measurements are listed in Table 2 for all modalities used in the experiment. Bold numbers in Table 2 indicate the highest CNR value among all imaging modalities.

From Table 2, we found that for the thin aluminum alloy (No.5) and glass (No.6) objects,

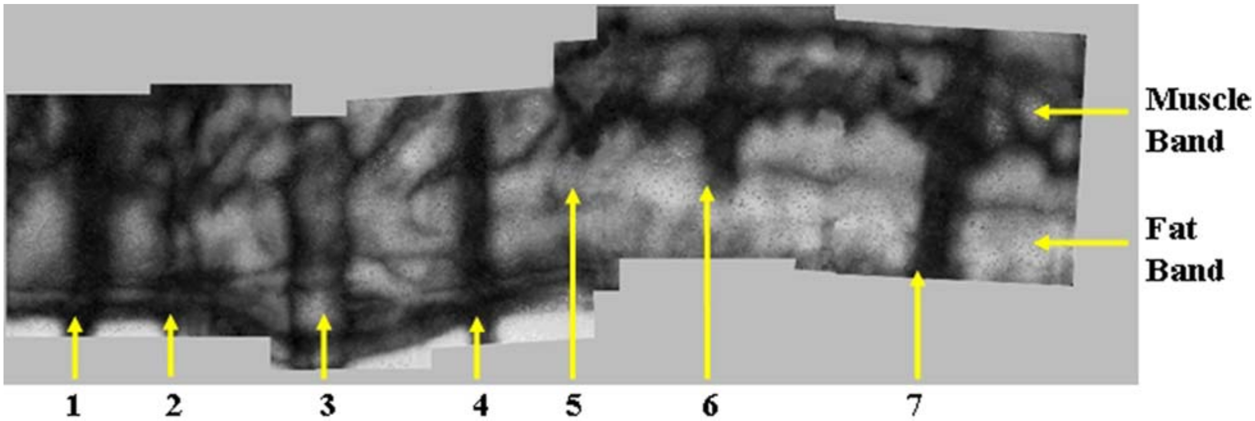

Figure 10. The stitched C-scan image of the porcine tissue sample containing the foreign objects. The arrows point to the locations of the foreign objects inserted in the porcine tissue and the numbers indicate the foreign objects according to Table 1.

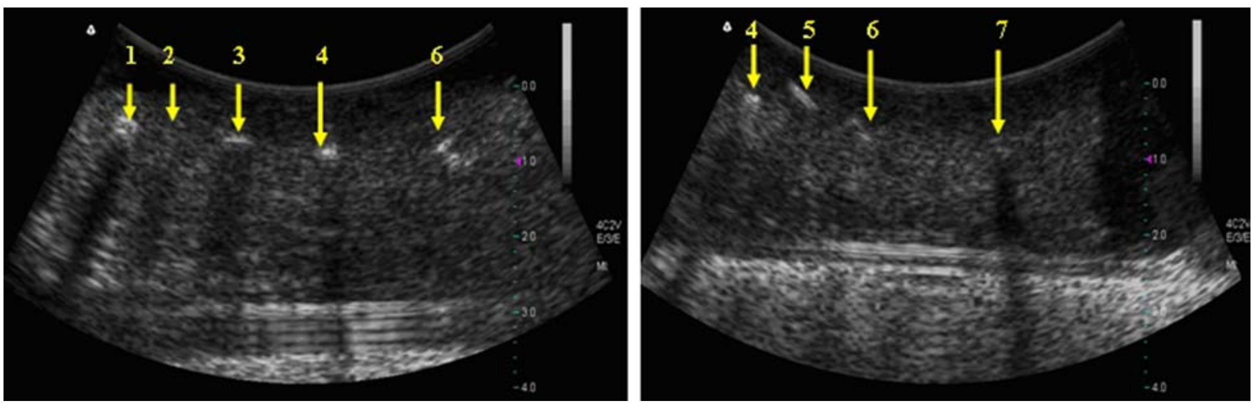

Figure 11. The B-scan ultrasound images of the porcine tissue with foreign objects. The arrows point to the locations of the foreign objects inserted in the porcine tissue. The numbers indicate the foreign objects and correspond to Table 1.

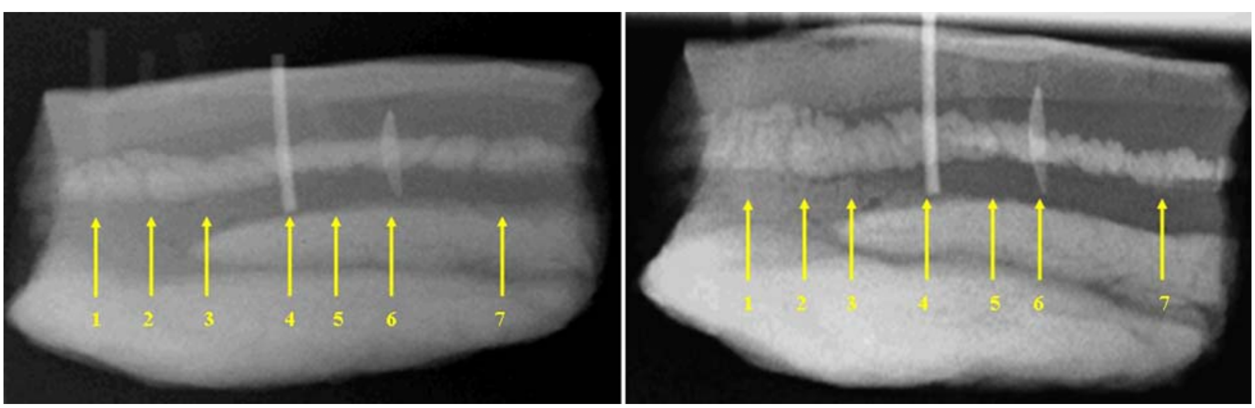

Figure 12. (A) The film-based radiograph obtained at 44kVP. (B) The CR image obtained at 40kVP. The arrows point to the locations of the foreign objects inserted in the porcine tissue. The numbers indicate the foreign objects corresponding to Table 1.

radiographs had highest CNR values of 3.46 (CR) and 8.43 (Film-based radiography) as compared to the ultrasound images; for the thicker aluminum alloy (No.4), the CNR values of both radiographs were also over 7. However, their performance in detecting objects Nos.1, 2, 3, and 7 was not considered as observable due to lower CNR values.

The C-scan ultrasound had four highest CNR values of the total seven foreign objects over the other modalities. The CNR value of the thicker aluminum alloy (No.4) and the glass object (No.6) in C-scan images reached 8.62 and 7.51 respectively. The B-scan ultrasound also had one highest value of 4.09 in detecting nylon (No.3). However, only a single cross section of each

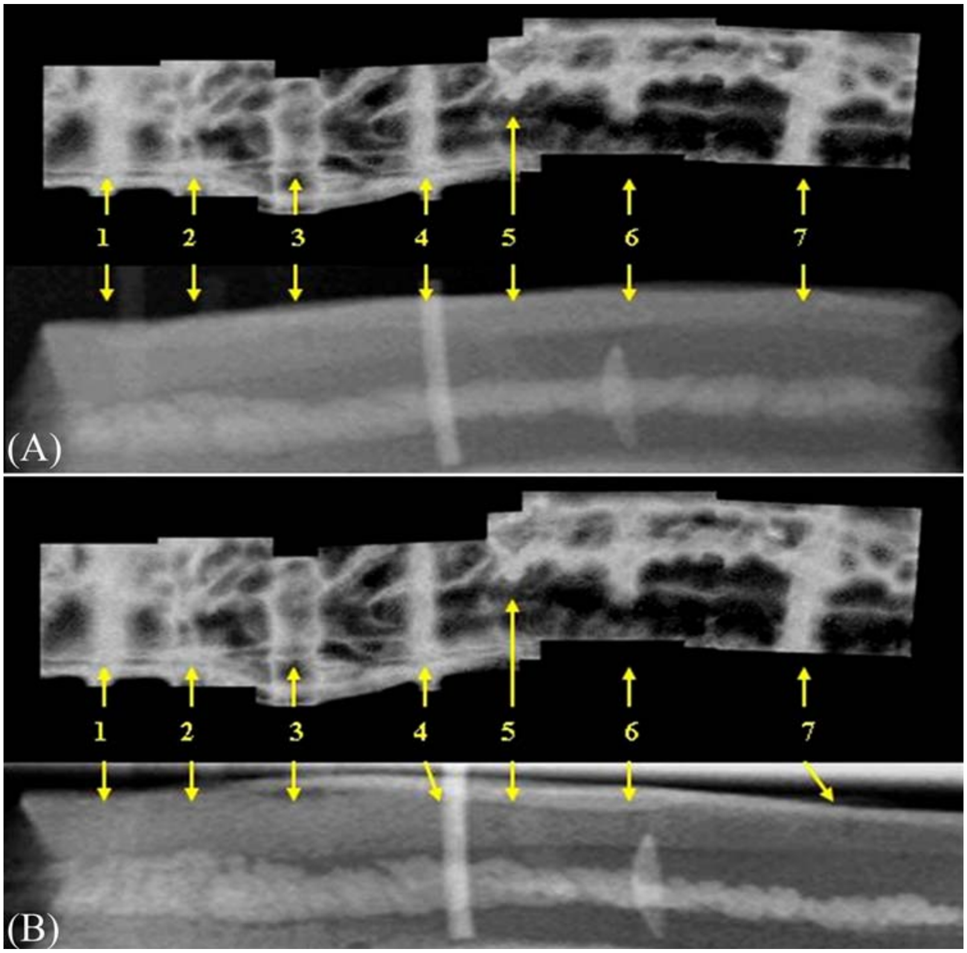

Figure 13. Displays of the inverted C-scan image with film-based radiograph and CR image: (A) C-scan image vs. film-based radiograph and (B) C-scan image vs. CR image. The numbers indicate the foreign objects corresponding to Table 1.

foreign object can be seen in the conventional B-scan image which makes it less favorable as a device for detecting foreign object in soft tissue. If we consider a CNR value of 1.5 as the contrast threshold, C-scan ultrasound images can clearly see the foreign objects except the thin aluminum alloy (No.5) whose acoustic attenuation is very close to the muscle.

5. DISCUSSION AND CONCLUSIONS

In this preliminary study, we investigated the conspicuity of seven foreign objects of various materials placed in a porcine soft tissue sample by using a C-scan ultrasound prototype, a portable B-scan ultrasound, a film-based radiography, and a computerized radiography. Acquired images were quantitatively analyzed to determine the conspicuity and CNR of the foreign objects.

Based on the visual comparisons and CNR analyses, we found that for film-based radiography and CR, aluminum alloys and glass possess highest CNR values; nevertheless, they were clearly visible in both C-scan and B-scan ultrasound images. The study demonstrated that bamboo, aluminum alloy (5182 series), heavy-weight polystyrene, nylon, and extra heavy-weight polystyrene objects were better detected by ultrasound imaging systems than radiography systems.

Comparatively, the C-scan images were speckle-free and did not have the same degree of geometric distortion as the conventional B-scan ultrasound images. Additionally, the structural features of the fat and muscle tissues in the porcine tissue sample were observable in the C-scan, but not in the B-scan images. According to the CNR analysis, the C-scan images had the highest values for four out of seven foreign objects and the three remaining objects were also clearly visible. Hence, the C-scan prototype can provide greater image quality and lead to better clinical detection for many types of foreign objects.

Ultrasound imaging has been widely used in medical diagnostic applications based on its real-time imaging ability, radiation-free, and non-invasive. The C-scan prototype described in this paper has been developed to combine the advantages of using ultrasound as a non-ionized source and a projection imaging geometry similar to conventional radiography. Based on the study results shown above, C-scan ultrasound imaging, when used for the detection of foreign objects in soft tissues, can be a useful tool in the care of patients with penetrating injuries, both for the detection of and as an interactive imaging tool to facilitate wound cleaning. Moreover, the PE-CMOS sensor array used for C-scan imaging will likely prove useful in other medical applications for its real-time, high resolution, high contrast, and fluoroscopy-like image display.

6. ACKNOWLEDGMENT

This project was supported in part by the US Army Medical Research and Materiel Command (Grant number: W81XWH-07-C-021).

7. REFERENCES

1. J-H Xuan, T Adali, Y Wang, E Siegel: Automatic detection of foreign objects in computed radiography. *J Biomed Optics* 5(4): 425-431 (2000)

2. J-J Hwang, J Quistgaard, J Souquet, L A Crum: Portable ultrasound device for battlefield trauma. *IEEE Proc Ultrason Symp* 2:1663-1667 (1998)

3. T D Boyse, D P Fessell, J A Jacobson, J Lin, M T Holsbeeck, C W Hayes: US of soft tissue foreign bodies and associated complications with surgical correlation. *Radiographics RSNA* 21(5):1251-1256 (2001)

4. T S Gibbs: The use of sonography in the identification, location, and removal of soft tissue foreign bodies. *J Diag Med Sono* 22(5):5-21 (2006)

5. S-C B Lo, D Rich, M E Lasser, J Kula, H Zhao, B Lasser, M T Freedman: C-scan transmission ultrasound based on a hybrid microelectronic sensor array and its physical performance. *SPIE Proc Med Img* 4325:89-95 (2001)

6. S-C B Lo, C-C Liu, M T Freedman, J Kula, B Lasser, M E Lasser ,Y Wang: Transmission and reflective ultrasound images using PE-CMOS sensor array. *SPIE Proc Med Img* 5750:69-76 (2005)

7. S-C B Lo, C-C Liu, M T Freedman, S-K Mun, J Kula, M Lasser, B Lasser, Y Wang: Projection-reflection ultrasound images using PE-CMOS sensor: a preliminary bone fracture study. *SPIE Proc Med Img* 6920(692005):1-8 (2008)

8. C-C Liu, S-C B Lo, M T Freedman, D Rich, M E Lasser, J Kula, B Lasser, J C Zeng, D Ro: Projection ultrasound and ultrasound CT using a PE-CMOS sensor: a preliminary study. *SPIE Proc Med Img* 5373:61-69 (2004)

9. C-C Liu, S-C B Lo, M T Freedman, Y Wang, D Rich, J Kula, B Lasser, M E Lasser: Transmission ultrasound computed tomography using a PE-CMOS sensor array: a preliminary animal study. *IEEE Int Symp Bio Img*: 908-911 (2006)

10. P A Lewin, H Busk: *In vivo* ultrasonic measurement of tissue properties. *Proc of 1982 IEEE Ultrason Symp* 709-712 (1982)

11. C F Njeh, D Hans, T Fuerst, C-C Glüer, H K Genant. Quantitative Ultrasound: Assessment of Osteoporosis and Bone Status. Martin Dunitz, London, UK (1999)

12. A R Selfridge: Approximate properties in isotropic materials. *IEEE Trans Son Ultrason* 32(3):381-387 (1985)

13. U Wegst: Bamboo and wood in musical instruments. *Annu Rev Mater Res* 38:323–349 (2008)

Abbreviations: PE-CMOS: piezoelectric material coated complementary metal-oxide semiconductor; CNR: contrast-to-noise ratio; CR: computerized radiography; ROIC: read-out integrated circuit; PVDF: polyvinylidene difluoride; US-CT: ultrasound c*omputerized tomography;*

Key Words: Projection ultrasound, C-scan ultrasound, PE-CMOS sensor array, Foreign objects detection, Soft tissue

Send correspondence to: Chu-Chuan Liu, ISIS Center, Department of Radiology, Georgetown University Medical Center, Washington, DC 20057, USA, Tel: 202-687-5135, Fax: 202-784-3479, E-mail: liu@isis.georgetown.edu

http://www.bioscience.org/current/vol2E.htm